CrystEngComm

Solvent diffusion through a non-porous crystal 'caught in the act' and related single-crystal-to-single-crystal transformations in a cationic dinuclear Ag(I) complex with 1,3-bis(imidazol-1-ylmethyl)-2,4,6-trimethylbenzene and BF4- as counterion

Journal:	*CrystEngComm*
Manuscript ID:	CE-ART-07-2015-001348.R1
Article Type:	Paper
Date Submitted by the Author:	06-Sep-2015
Complete List of Authors:	Alen, Jo; KU Leuven, Chemistry Van Meervelt, Luc; KU Leuven, Chemistry Dehaen, Wim; KU Leuven, Chemistry Dobrzanska, Liliana; KU Leuven, Chemistry

CrystEngComm

ARTICLE

Solvent diffusion through a non-porous crystal 'caught in the act' and related single-crystal-to-single-crystal transformations in a cationic dinuclear Ag(I) complex with 1,3-bis(imidazol-1-ylmethyl)-2,4,6-trimethylbenzene and BF_4^- as counterion

Received 09th July 2015

DOI: 10.1039/x0xx00000x

www.rsc.org/

Jo Alen,[a] Luc Van Meervelt[a], Wim Dehaen[a] and Liliana Dobrzańska[a*]

The effect of a range of solvents on non-porous single-crystals of a cyclic, dinuclear silver(I) complex with 1,3-bis(imidazol-1-ylmethyl)-2,4,6-trimethylbenzene (**bitmb**) of the formula $[Ag_2(\mathbf{bitmb})_2](BF_4)_2$ (**1**) was investigated by single-crystal X-ray diffraction studies. It allowed us to get a few snapshots of the process of solvent diffusion through the crystal, connected with a series of reversible transformations. We have isolated disolvated **2a** and monosolvated **2b** forms with acetonitrile, monosolvated forms **3b** and **4b** with acetone and ethanol respectively, as well as a monosolvated form **4c** with ethanol which is an intermediate between **1** and **4b**. Longer exposure of the crystals to solvent vapours leads to the formation of a polymeric 1D Ag(I) complex of general formula $[Ag\mathbf{bitmb}(BF_4)]_n$ (**5**).

Introduction

Single-crystal-to-single-crystal transformations (SC-SC) allow us to follow in situ structural changes triggered by different types of stimuli such as temperature[1], pressure[2], solvents[3], counterions[4] or even metal ions[5], which can also be replaced/captured in SC-SC fashion in the case of coordination compounds. These types of studies expand our knowledge concerning structure-properties relationships, which in turn leads to proper, rational design of materials of desired properties. The literature concerning the occurrence of SC-SC has been growing in the past couple of years, partly as the result of hardware progress. However, the majority of the reports are devoted to the alterations taking place in polymeric coordination compounds, especially metal-organic frameworks.[6] Molecular organic crystals or discrete metal-organic complexes do not gain so much attention, being perceived as more difficult to survive the transformations, which is connected with the presence of weaker interactions between the molecules. However, this could also be turned into an advantage, as it could lead to higher molecular flexibility.[7] Investigating the response of crystals of discrete molecules to different types of external stimuli, we have revealed for example a series of guest-induced interconversions, taking place in a crystal of a neutral, dinuclear Cu(II) complex, that involve positional and conformational changes[8]. Recently, we also revealed conformational switching (1,3-alternate ↔ 1,2-alternate), induced by solvent, taking place in a single-crystal of homodithiacalix[4]arene[9]. Continuing our work on SC-SC, we would like to present here solvent-induced transformations taking place in a single-crystal of $[Ag_2(\mathbf{bitmb})_2](BF_4)_2$. The study allows us to gain some valuable insight into the transport of solvent molecules through this seemingly non-porous crystal.

Studying the mechanism of guest diffusion through crystalline material is an important topic, as gaining control over this process would facilitate the design of materials of desired porous properties. However, the phenomenon, especially in the case of non-porous crystals, is still poorly recognized and it might be that its complexity and uniqueness will never fit into a general scheme. For the moment, there are some hypotheses explaining for example the transport processes in *p*-tert-butylcalix[4]arene (which involves rotation of the *tert*-butyl groups and translational sliding of the bilayers)[10], hydroquinones (via a flipping, or swapping, mechanism involving hydroxyl hydrogen-bonded rings[11] or via a rubber-band mechanism[12]). The latter was also postulated for Dianin's compound.[12]

By exposing the single-crystal of the title Ag(I) complex to a range of solvents, we have isolated 3 distinct forms in SC-SC fashion. These structures illustrate well how complicated and unexpected the process of solvent uptake can be.

[a]*Department of Chemistry, Katholieke Universiteit Leuven, Celestijnenlaan 200F, 3001 Heverlee, Belgium.E-mail: lianger@chem.kuleuven.be.*

†Dedicated to Professor A. J. Leno on the occasion of his birthday.

† Electronic Supplementary Information (ESI) available: preparative and crystallographic details for $[Ag_2(bitmb)_2](SbF_6)_2]$, a table presenting the effect of counterions on the shape of the metallocycles formed, unit cell parametes for **5**, and a figure with overlay of **1** and the corresponding metallocycle from **4c**. CCDC reference numbers 1411588-1411593. See DOI: 10.1039/x0xx00000x

Experimental

Reagents and materials

The ligand 1,3-bis(imidazol-1-ylmethyl)-2,4,6-trimethylbenzene (**bitmb**), was synthesised by the S_N2 substitution reaction of imidazole with 2,4-bis(chloromethyl)-1,3,5-trimethylbenzene, as reported previously.[13b] ^{1}H NMR ($CDCl_3$, 600 MHz) δ 7.31 (s, 2H), 7.04 (s, 1H), 7.03 (t, 2H, J = 1 Hz), 6.74 (t, 2H, J =1 Hz), 5.15 (s, 4H), 2.33 (s, 6H), 2.20 (s, 3H); ^{13}C NMR ($CDCl_3$, 150 MHz) δ 138.6, 137.8, 136.5, 131.4, 130.0, 129.5, 118.4, 45.2, 19.9, 15.3. Anal. calcd for $C_{17}H_{20}N_4 \cdot H_2O$: C, 68.43; H, 7.43; N, 18.78%, found: C, 68.30; H, 7.54; N, 18.75%.

Synthesis of $[Ag_2(bitmb)_2](BF_4)_2$ (1)

A solution of 0.1 mmol $AgBF_4$ in acetonitrile (10 mL) was added to a solution of 0.1 mmol **bitmb** in acetonitrile (25 mL). The mixture was stirred for a few minutes and left in a dark environment for slow evaporation. After three weeks, colourless crystals suitable for single-crystal X-ray diffraction studies were obtained.

Preparation of the crystals

The single-crystal-to-single-crystal transformations were achieved by immersing a single-crystal of **1** into a solvent or by leaving the single-crystal of **1** in the vapour of a particular solvent overnight or for a longer period (specified further on in the paper). Immersion of the crystal in the solution causes more rapid transformations, leading to worse quality crystals. Immersion of a crystal of **1** in acetonitrile for longer than 2 minutes causes fragmentation of the crystal. Starting from **1**, we have isolated 5 new solvates, namely: $[Ag_2(\mathbf{bitmb})_2](BF_4)_2 \cdot 2CH_3CN$ (**2a**), $[Ag_2(\mathbf{bitmb})_2](BF_4)_2 \cdot CH_3CN$ (**2b**), $[Ag_2(\mathbf{bitmb})_2](BF_4)_2 \cdot (CH_3)_2CO$ (**3b**), $[Ag_2(\mathbf{bitmb})_2](BF_4)_2 \cdot C_2H_5OH$ (**4b**), $[Ag_2(\mathbf{bitmb})_2](BF_4)_2 \cdot C_2H_5OH$ (**4c**). It is worth mentioning that the crystals of **1** are not affected by water from the environment, as was checked after exposure to the atmosphere for 6 months.

Structure determination

The single-crystal X-ray diffraction data were collected on an Oxford Diffraction SuperNova diffractometer with Eos CCD detector, MoK_α radiation, λ = 0.71073 Å. Data frames were processed (unit cell determination, intensity data integration, correction for Lorentz and polarization effects, and empirical absorption correction) using the corresponding diffractometer's software package.[14a] Each structure was solved by direct methods using SHELXS-97 and refined by full-matrix least-squares methods based on F^2 using SHELXL-97[14b]. The programs MERCURY[14c] and POV-Ray[14d] were used to prepare the molecular graphics images. All non-hydrogen atoms were refined anisotropically, and the hydrogen atoms were placed in calculated positions with displacement factors fixed at 1.2 times U_{eq} of the parent C atoms and 1.5 times U_{eq} for methyl groups with C-H = 0.95 (aromatic), 0.98 (methyl) and 0.99 Å (methylene). In **1** and **2a,** geometrical and anisotropic displacement parameter restraints were applied to the counterions. The ethanol molecules in **4b** and **4c** were found to be disordered and modelled into two orientations. The H atoms (O-H) in **4b** and **4c** were located in a difference map and refined with restrained O–H bond lengths. The crystals' quality of **4c** and **5** resulted in poor datasets. Therefore, we did not deposit those structures with CCDC. However, as the results were significant for the paper, we discussed them in the main text.

Applying the SQUEEZE instruction of PLATON confirmed the presence of the number of solvent molecules given.[14e] Because the process is taking place so quickly, thermal analyses could not be performed.

A summary of the data collection and structure refinement parameters is provided in Table 1.

Results and discussion

In one of our previous reports concerning metal complexes with **bitmb**[13], we presented the effect of counterions on the formation of silver(I) complexes with metal to ligand ratio 1 to 1.[13b] Therein we have also demonstrated that seemingly non-porous discrete metallocyclic complexes $[Ag_2(\mathbf{bitmb})_2](SbF_6)_2$ and $[Ag_2(\mathbf{bitmb})_2](PF_6)_2$ are able to undergo reversible single-crystal-to-single-crystal transformations upon uptake/release of acetonitrile molecules. In the present study, we have investigated the effect of a range of solvents, namely acetonitrile, acetone and ethanol on single-crystals of a related, new dinuclear $[Ag_2(\mathbf{bitmb})_2](BF_4)_2$ complex (**1**).

Crystal structure of $[Ag_2(bitmb)_2](BF_4)_2$ (1)

The crystal structure of complex **1** is reminiscent of the structures of analogous **bitmb** complexes with counterions PF_6^- and NO_3^- (previously reported by our group) as well as SbF_6^-, for which we were able to collect the full data set in meantime (see SI for the preparation, the crystallographic data and the refinement parameters). The dinuclear Ag(I) compound **1** crystallises in the triclinic centrosymmetric space group $P\bar{1}$ with half a cationic Ag(I) complex, consisting of a silver ion located on a general position and one **bitmb** ligand, and two crystallographically independent counterions with half occupancy each (as they were found disordered around an inversion centre) in the asymmetric unit (Fig. 1).

It is worth noting the absence of disorder in the case of the larger counterions SbF_6^- and PF_6^- with octahedral geometry, and its occurrence in the case of a smaller, trigonal NO_3^- counterion (to follow the effect of the counterion on the size/shape of the metallocycle, see Table S1).

The silver ions in the metallocycle are coordinated in a linear fashion (N–Ag–N = 174.1 (1)°) to N atoms of imidazole rings originating from two distinct, bridging **bitmb** ligands in *syn* conformation. The distance between two silver ions forming a box is 7.170 Å. The mesitylene rings are oriented almost orthogonally to the plane of the metallocycle, defined by N17-N3-N17'-N3', with an angle of 84.77°. As a result of the

symmetry of the cationic metal complex, the mesitylene rings present in the cyclic unit are pointing opposite directions. The imidazole rings are directing to the middle of the metallocycle with angles between the planes of imidazole rings on the same ligand of 40.26°. One of the disordered counterions is trapped in the centre of the metallocycle.

In the packing arrangement, we can distinguish layers of stacked metallocyclic units in the *ab* plane, which are separated by counterions (Fig. 2). Simplified, they can be considered as tilted columns of metallocycles stacked along the *b* axis, held together by C-H···F interactions (whereby F is originating from the counterion encapsulated in the ring) with distances between the silver ions of adjacent complexes of 9.441 Å, that are extended into rows along the *a* direction by stacks of metallocycles held together via C-H···π interactions (C13-H13B···(N1-C5); C···centroid distance of 3.622(6) Å and C-H-centroid angle of 143°) with an adjacent Ag···Ag distance of 8.974 Å.

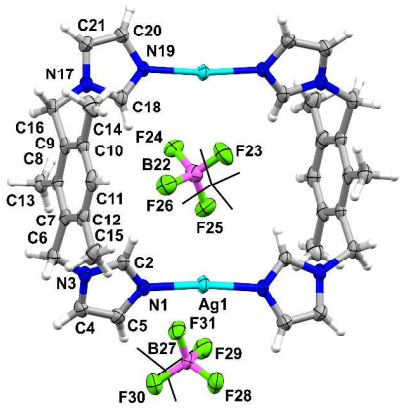

Fig. 1 Atomic displacement plot showing **1** (50% probability). Unlabelled atoms are related to the labelled atoms by the symmetry operations -*x*, 1-*y*, 1-*z* for the metallocycle and encapsulated BF_4^-, and 1-*x*, 2-*y*, 2-*z* for the other counterion; the same labelling applies to **2a**.

As mentioned, the couterions occupying the interstitial spaces are also disordered and interact weakly by C-H···F interactions with the layers of metal complexes surrounding them. The distances between Ag···Ag ions of cyclic units from adjacent layers guarded by BF_4^- ions are 5.453 Å.

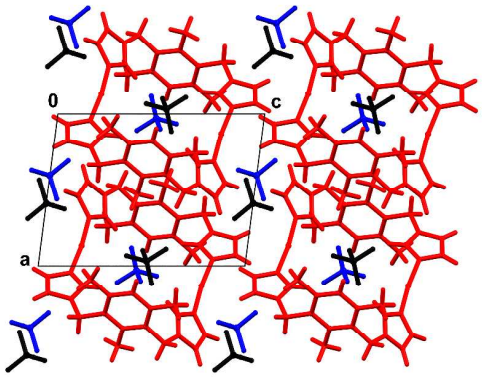

Fig. 2 Packing arrangement of **1** projected down the b axis, with parallel layers of metallocycles in the *ab* plane coloured red and disordered counterions in black and blue.

Crystal structure of $[Ag_2(bitmb)_2](BF_4)_2{\cdot}2CH_3CN$ (2a)

Immersion of a crystal of **1** in acetonitrile for 2 minutes or leaving it in acetonitrile vapour for a week allowed us to isolate the disolvated form **2a**, similar to the disolvates of the complexes with counterions SbF_6^- and PF_6^-. However, the difference in geometry and the size of the counterion in **2a** once again accounts for disorder, which also influences the stability of the solvate formed. If not held under a steady stream of liquid nitrogen, **2a** transforms back to **1** within a couple of minutes. This was not the case for the compounds with SbF_6^- and PF_6^- counterions, whereby the disolvated forms were stable for weeks. After solvent uptake, the centrosymmetric triclinic crystal structure is maintained and its main features at first glance have not changed much (Fig. 3). The dinuclear Ag(I) complex **2a** shows a similar conformation as in **1** (see Figure 4) with an Ag···Ag distance of 7.167 Å and an angle N-Ag-N of 175.2(2)°. As previously, the inversion centre is located in the middle of the cyclic unit. There are two distinct counterions present, one of which is trapped in the metallocycle as before, and the other one is located in the space formed between the layers of metallocycles. However, this space has expanded to accommodate the acetonitrile molecules. The appearance of solvent influences simultaneously the unit cell parameters, mostly the *c* axis, causing its elongation of *ca*. 1.6 Å in comparison with **1** (see Table 1).

A closer look at the packing arrangement indicates that the solvent uptake is accompanied by the reorientation of the layers leading to an alignment of silver ions from adjacent layers (Fig. 3). The distance between silver ions from metallocycles separated by solvent molecules is 6.257 Å, meaning an increase of 0.8 Å compared with the corresponding distance in **1**. The silver ions from adjacent molecules stacked along the *b* axis are slightly further apart (Ag···Ag is 9.667 Å), but closer for those stacked along the *a* axis (Ag···Ag is 8.730 Å). However, in general, the interactions between the molecules are not much affected.

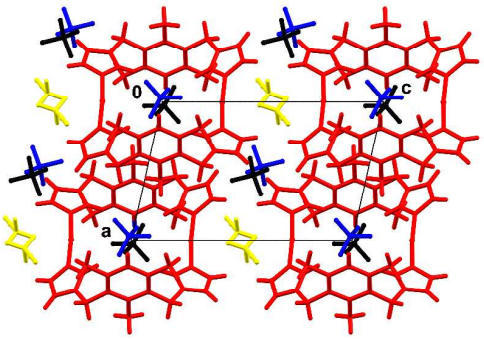

Fig.3 Packing arrangement of **2a** projected down the *b* axis, with layers of metallocycles in the *ab* plane coloured red, disordered counterions in black and blue, and acetonitrile molecules in yellow.

The solvent molecules are occupying separate voids, which can only be mapped as continuous channels with a spherical probe radius below 1.1 Å (solvent accessible surface). The acetonitrile molecules are located in close proximity of the Ag ions (N···Ag is 3.000(6) Å) and also further interact with the cationic metal complexes via C-H···N interactions involving C5 and C20 of the imidazole rings originating from cyclic units from adjacent layers and N from the solvent molecule. There are also some short C-H···F type contacts with the counterions occupying the interstitial spaces.

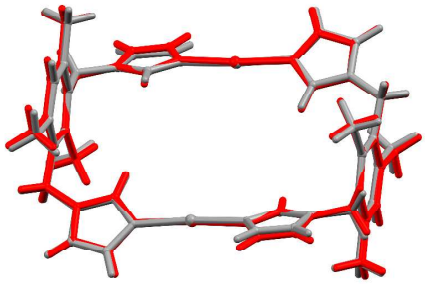

Fig. 4 Overlay of the metallocycles **1** (grey) and **2a** (red), with the silver ions represented as balls; r.m.s. deviation is 0.1198 Å.

Crystal structure of $[Ag_2(bitmb)_2](BF_4)_2 \cdot CH_3CN$ (2b)

As mentioned before, the solvent molecules are not strongly retained in the crystal of **2a**, which readily returns to the solvent-free form **1** if exposed to air for a couple of minutes. However, by leaving the crystal **2a** for 1 min in air, we were able to isolate a partially solvent loaded form **2b**. The same form, showing the presence of only one molecule of acetonitrile per metallocycle, could be obtained by immersing a crystal of **1** in acetonitrile for 30 seconds or leaving it overnight in acetonitrile vapour.

2b also belongs to the centrosymmetric triclinic space group P$\bar{1}$ and shows the presence of one metallocyclic cationic complex, two counterions and one acetonitrile molecule in the asymmetric unit. The cationic Ag(I) complex itself is not centrosymmetric anymore, meaning that its conformation has changed, causing deformation of the metallocycle compared with **1** and **2a**. This is evident from the orientation of the imidazole rings, especially those containing N19 and N22 (see Fig. 5). The geometry around the silver ions slightly deviates from linearity with N1-Ag1-N40 and N19-Ag2-N22 angles of 172.1(2)° and 174.0(2)° respectively. The angles between the planes of opposite imidazole rings are 17.50° and 42.22° for the pairs N1/N19 and N22/N40 respectively and the angle between the planes of the mesitylene rings and the plane of the metallocycle, defined as before, are 89.7 and 81.3°. The Ag···Ag distance in the box is 7.045 Å, which is slightly shorter than that in **1** and **2a**.

One of the counterions again is trapped in the middle of the metallocycle and the other one is located between the layers of metallocycles in close proximity to Ag2 (F51···Ag2 is 3.187(3) Å). None of the counterions is disordered this time. The acetonitrile molecules are located between the layers of metallocycles in the space guarded by the silver ions (with an Ag···Ag separation of 6.752 Å; i.e. an increase of *ca*. 0.5 Å compared with **2a**), the imidazole rings from metallocycles originating from adjacent columns of distinct layers and BF_4^- counterions. Each acetonitrile molecule stays in close proximity to Ag1 with an N-Ag distance of 3.193(8) Å. Comparison of the packing diagrams of **2b** and **2a** indicates that the solvent molecules in **2b** are located in every second space between the columns of metallocycles (Fig. 6). As a result of molecular rearrangements, the Ag···Ag distance between solvent-free spaces is 4.072 Å, which is much shorter (*ca*. 1.4 Å) than the corresponding distance in **1**. Furthermore, the pore formed in **2b** is bigger than in **2a** and it can be mapped as a continuous channel with a spherical probe radius below 1.22 Å (solvent accessible surface).

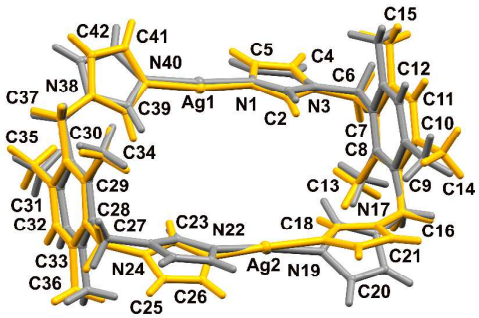

Fig. 5 Overlay of metallocycles **1** (grey) and **2b** (orange, labelled), illustrating loss of an inversion centre by the cyclic unit shown in orange at this stage of the solvation/desolvation process; r.m.s. deviation is 0.4980 Å .

Morever, the deformation of the metal complex leads to a series of molecular rearrangements in the layers, whereby the molecules still stack nicely in columns along the *a* axis held by weak C-H···F interactions, with distances between the silver ions from adjacent molecules of 10.146 Å. However, as the adjacent columns in the layer are related by an inversion center, they do not form linear rows anymore and the distances between adjacent silver ions alternate between values of 8.200 Å and 8.871 Å.

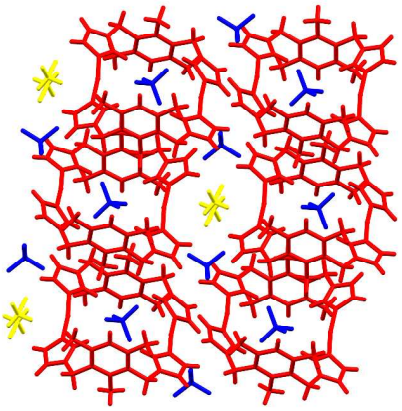

Fig. 6 Packing arrangement in **2b** projected down the *a* axis demonstrating the uptake of the first molecule of acetonitrile, with the layers of the metallocycles shown in red, counterions in blue, and solvent in yellow.

Crystal structure of $[Ag_2(bitmb)_2](BF_4)_2$·acetone (3b)

The immersion of **1** in acetone for 2 minutes or exposure of **1** to acetone vapour overnight resulted in the transformation of **1** to **3b**, which matches well with the crystal structure **2b** (the unit cell parameters are almost the same, see Table 1). The transformation is reversible, returning to **1** in just a couple of minutes. We were not able to isolate a disolvated structure corresponding to **2a**. Most likely the bulky shape and size of the acetone molecules (having a molecular volume of 64 $Å^3$ compared with 49 $Å^3$ for acetonitrile) prohibits further rearrangements needed for the formation of the pores to accommodate the second solvent molecule (Fig. 7). The silver ions' distance between the columns of adjacent layers increases with *ca.* 0.2 Å in comparison with **2b** (value of 6.917 Å). The conformations of **2b** and **3b** stay more or less the same (r.m.s. deviation of 0.1237 Å). The oxygen atom from the acetone molecule is located at a distance of 3.211(6) Å from Ag1. Acetone interacts more intensely with the counterions located between the layers than acetonitrile in **2b**, involving both methyl groups in C-H···F interactions. There are also other contacts formed with the metallocycles that involve the methyl groups and the O atom from the solvent molecule.

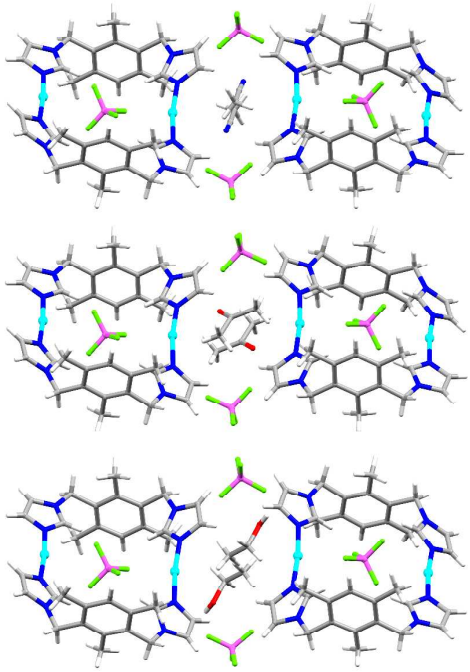

Fig.7 Plots representing the orientation of the solvent molecules in the pores of the monosolvated forms **b**, projected down the *a* axis. From top to bottom: acetonitrile (**2b**), acetone (**3b**) and ethanol (**4b**, the disorder of the ethanol molecules omitted for clarity).

Crystal structures of $[Ag_2(bitmb)_2](BF_4)_2$·EtOH (4b)

Immersion of **1** in ethanol for 1 minute or its exposure to ethanol vapour for two nights resulted in the transformation of **1** to **4b**. The transformation is reversible and, in a couple of minutes, the crystal is going back to **1**. The crystal structure of **4b** is isostructural with **2b** and **3b**. Once again we did not succeed in isolating a disolvated form, which we assume is due to the angular shape of the solvent, which is only slightly bigger than acetonitrile (molecular volume of 54 $Å^3$) (Fig. 7). The conformation of the metallocycle doesn't really change (overlay with **2b** – r.m.s. deviation is 0.0780 Å). The distance between the silver atoms from metallocycles located in adjacent layers is 6.629 Å, which is even slightly shorter (*ca.* 0.1 Å) than in **2b**. The solvent molecules are disordered over two positions with the O atom staying in the vicinity of Ag1 (3.354(6) Å). They are less involved in intermolecular interactions than acetone, forming O-H···F hydrogen bonds with the adjacent counterion and a weak C-H···N hydrogen bonding with the closest metallocycle (whereby C-H is originating from a methylene group of the solvent).

Crystal structures of $[Ag_2(bitmb)_2](BF_4)_2$·EtOH (4c)

Checking the reversibility of the transformation from **4b** to **1**, we have identified one more form, namely **4c**, which we believe is an intermediate between the former two. The crystal quality was very poor, but we succeeded to solve the crystal structure and get a satisfying model. The single-crystal went through much bigger changes than those observed for the previous forms. The symmetry of the crystal, has altered from the triclinic P$\bar{1}$ to the monoclinic *C*2/*c* space group. In the asymmetric unit, there are two halves of crystallographically distinct metallocycles with the **bitmb** ligand and a silver ion located on general positions, two counterions encapsulated in these two cyclic units with half occupancy each (as the corresponding B atoms are located on special positions, such as an inversion centre in the Ag1 containing metallocycle, and a two-fold axis for the one with Ag2), one counterion occupying the interstitial space between the metallocycles located on a general position, and a disordered molecule of ethanol modelled into two orientations. The metallocyclic units (Ag1) correspond quite well with those present in **1** (r.m.s. deviation of 0.1437 Å, see Fig. S1). More special is the other metallocycle (Ag2), the conformation of which to our surprise differs not only by changes in the position of the imidazole rings, but also by the orientation of the mesitylene rings which are pointing in the same direction (Fig. 8).

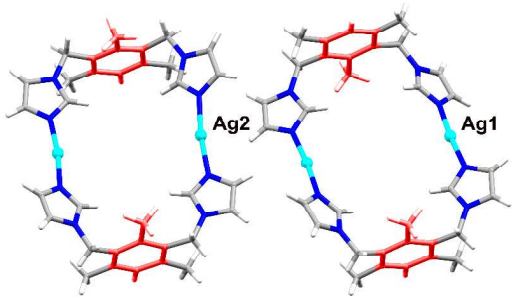

Fig. 8 Representation of the two distinct metallocycles present in **4c**, with the mesitylene rings (in red) adopting different orientations.

Further comparison of these two metallocycles indicates other smaller changes such as the Ag···Ag distance or the angle between the planes of opposing imidazole rings in the cyclic unit which are 7.056 Å/50.77° for Ag1 and 7.245 Å/34.20° for Ag2. The coordination geometry of the silver ions does not differ much between these two units, with N-Ag-N' angles of 172.1(4)° and 174.8(4)° for Ag1 and Ag2, respectively.
An overlay of both metallocycles present in **4c** (see Fig. 9), could indicate that the deformation of the metallocycle observed in the **b** forms is an effect remaining from the rotation/swinging of the mesitylene rings during the preceding step.

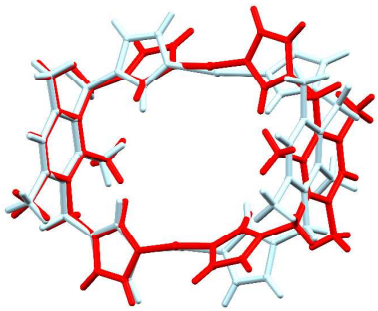

Fig. 9 Overlay of both metallocycles present in **4c**.

The ethanol molecules are occupying more or less the positions which were initially taken by one of the disordered counterions in **1** (see Fig. 10). The remaining counterion is well ordered. The Ag···Ag distances originating from the cyclic units from the adjacent layers in which molecules do no longer stack so orderly as in **1** or **2a** are 5.341 Å, which is only *ca*. 0.1 Å shorter than in **1**.
It looks like the solvent molecules are taking advantage of the free space available in the crystal caused by the disordered counterions and are pushing their way between the layers. This obviously does not take place without molecular response of the metal complexes, namely rearrangements/conformational changes leading to further uptake without damaging the single-crystals. However, we are fully aware that what we present are merely a couple of snapshots from a very complicated continuous process.

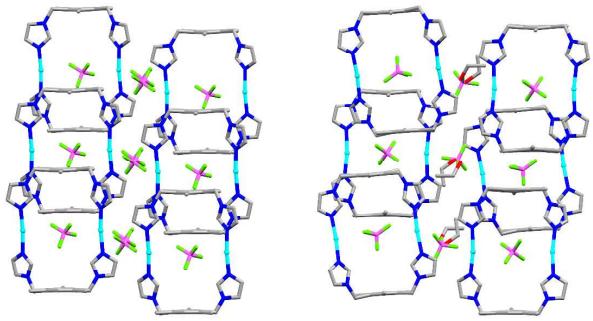

Fig. 10 Packing representation of **1** in the direction [-1-10] (left; disordered counterions present between the layers) and **4c** in the direction [010] (right; ethanol in grey and red accommodated between the layers) showing most likely the starting stage of the crystal penetration by the solvent molecules.

Crystal structure of $[Agbitmb(BF_4)]_n$ (5)

It is worth noting that longer exposure of complex **1** to the vapour of all three solvents (over 1 month) causes regrowing of the crystals, which results in the formation of a polymeric 1D wave-like Ag(I) complex (Fig. 11). The crystal quality was very poor, but good enough to get an idea about the crystal structure formed (for unit cell parameters, see Table S3). It crystallises in a monoclinic system of the *C*2/*c* space group and shows the presence of two distinct silver ions in the asymmetric unit which are located on special positions with an occupancy of half each (Ag1 is located on a two-fold axis and Ag2 on an inversion center), one **bitmb** ligand and one counterion. The silver ions are coordinated via N atoms of the imidazole rings originating from the bridging **bitmb** ligands in *syn*-conformation. The geometry around the silver ions (N-Ag-N) remains linear, yet is slightly deformed around Ag1 with an angle of 169° (180° around Ag2).

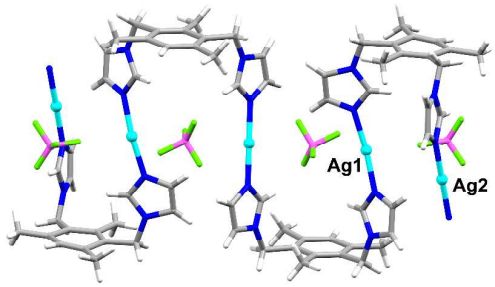

Fig. 11 Fragment of the wave-like chain in **5** extending along the *c* axis; disorder of the counterions not shown for clarity.

Conclusions

The presented results show that in some cases solvent diffusion through a non-porous crystal can be more complicated than could initially be expected. Having revealed only two structures of the presented system, namely the solvent-free (**1**) and disolvated (**2a**) form, one could easily draw the wrong conclusion that the process is rather simple. As the molecular structures of the Ag(I) complex in these two forms stay more or less the same, we could assume that the process is based on minor rearrangements involving the layers consisting of metallocycles in the crystal lattice. However, deeper insight into the process reveals that switching from form **1** to **2a** and back actually involves a few intermediate steps including the formation of monosolvated forms. The transformations taking place engage not only a rearrangement of the molecules, but also conformational changes of the metal complexes, such as a swinging of the mesitylene rings or flapping of the imidazole rings, to facilitate the diffusion

process. All this happens in a very short time, in a concerted fashion, in a single-crystal and it could be very easily overlooked for this system, as the solvent molecules are just traversing by the crystal and do not form stable solvates. Moreover, the size/shape of the solvent molecules is crucial in the loading process. Further studies, aimed at better understanding of guest diffusion are being undertaken, including the use of larger solvent molecules, with different H bonding capacities.

Acknowledgements

We thank the Hercules Foundation for supporting the purchase of a diffractometer through project AKUL/09/0035.

References

1 (a) Q.-Q. Li, C.-Y. Ren, Y.-Y. Huang, J.-L. Li, P. Liu, B. Liu, Y. Liu and Y.-Y. Wang, *Chem. Eur. J.*, 2015, **21**, 4703-4711; (b) R. G. D. Taylor, B. R. Yeo, A. J. Hallett, B. M. Kariuki and S. J. A. Pope, *CrystEngComm*, 2014, **16**, 4641-4652; (c) M. C. Bernini, F. Gándara, M. Iglesias, N. Snejko, E. Gutiérrez-Puebla, E. V. Brusau, G. E. Narda and M. Á. Monge, *Chem. Eur. J.*, 2009, **15**, 4896-4905.
2 H. Jin, A. M. Plonka, J. B. Parise and N. S. Goroff, *CrystEngComm*, 2013, **15**, 3106-3110.
3 (a) Y.-C. He, J. Yang, Y.-Y. Liu and J.-F. Ma, *Inorg. Chem.*, 2014, **53**, 7527-7533; (b) L. Wen, P. Cheng and W. Lin, *Chem. Commun.*, 2012, **48**, 2846-2848; (c) Z.-M. Hao and X.-M. Zhang, *Dalton Trans.*, 2011, **40**, 2092-2098.
4 N. Li, F. Jiang, L. Chen, X. Li, Q. Chen and M. Hong, *Chem. Commun.,* 2011, **47**, 2327-2329.
5 (a) S. Sen, S. Neogi, K. Rissanen and P. K. Bharadwaj, *Chem. Commun.*, 2015, **51**, 3173-3176; (b) J. Tian, L. V. Saraf, B. Schwenzer, S. M. Taylor, E. K. Brechin, J. Liu, S. J. Dalgarno and P. K. Thallapally, *J. Am. Chem. Soc.*, 2012, **134**, 9581-9584.
6 (a) C.-P. Li, J. Chen, C.-S. Liu and M. Du, *Chem. Commun.,* 2015, **51**, 2768-2781; (b) J.-P. Zhang, P.-Q. Liao, H.-L. Zhou, R.-B. Lin and X.-M. Chen, *Chem. Soc. Rev.,* 2014, **43**, 5789-5814; (c) Z. Yin and M. H. Zeng, *Sci. China Chem.,* 2011, **54**, 1371-1394; (d) J. J. Vittal, *Coord. Chem. Rev.*, 2007, **251**, 1781-1795; (e) M. Kawano and M. Fujita, *Coord. Chem. Rev.*, 2007, **25**, 2592-2605.
7 (a) M. du Plessis, V. J. Smith and L. J. Barbour, *CrystEngComm*, 2014, **16**, 4126-4132; (b) T. Jacobs and L. J. Barbour, *CrystEngComm*, 2013, **15**, 1512-1514; (c) S. H. Lim, M. M. Olmstead and A. L. Balch, *Chem. Sci.*, 2013, **4**, 311-318; (d) J. T. A. Jones, D. Holden, T. Mitra, T. Hasell, D. J. Adams, K. E. Jelfs, A. Trewin, D. J. Willock, G. M. Day, J. Bacsa, A. Steiner and A I. Cooper, *Angew. Chem. Int. Ed.*, 2011, **50**, 749-753; (e) C. Massera, M. Melegari, E. Kalenius, F. Ugozzoli and E. Dalcanale, *Chem. Eur. J.*, 2011, **17**, 3064-3068; (f) S. M. Mobin, A. K. Srivastava, P. Mathur and G. K. Lahiri, *Dalton Trans.*, 2010, **39**, 1447-1449; (g) A. Deák, T. Tunyogi, Z. Károly, S. Klébert and G. Pálinkás, *J. Am. Chem. Soc.*, 2010, **132**, 13627-13629.
8 L. Dobrzańska, G. O. Lloyd, C. Esterhuysen and L. J. Barbour, *Angew. Chem. Int. Ed.*, 2006, **45**, 5856-5859.
9 J. Thomas, G. Reekmans, P. Adriaensens, L. Van Meervelt, M. Smet, W. Maes, W. Dehaen and L. Dobrzańska, *Angew. Chem. Int. Ed.*, 2013, 52, 10237-10240.
10 (a) X. Gu, L. Zhang, X. Gong, W. M. Lau and Z. F. Liu, *J. Phys. Chem. B*, 2008, **112**, 14851-14856; (b) J. L. Atwood, L. J. Barbour, A. Jerga and B. L. Schottel, *Science*, 2002, **298**, 1000-1002.
11 J. L. Daschbach, T.-M. Chang, L. R. Corrales, L. X. Dang and P. McGrail, *J. Phys. Chem. B,* 2006, **110**, 17291-17295.
12 A. Nemkevich, M. A. Spackman and B. Corry, *Chem. Eur. J.*, 2013, **19**, 2676-2684.
13 (a) L. Dobrzańska, *Inorg. Chem.Commun*., 2015, **55**, 21-24; (b) L. Dobrzańska, *CrystEngComm*, 2011, **13**, 2303-2309; (c) C. E. Strasser, L. Dobrzańska, H. Schmidbaur, S. Cronje and H. G. Raubenheimer, *J. Mol. Struct*., 2010, **977**, 214-219; (d) L. Dobrzańska, G. O. Lloyd, H. G. Raubenheimer and L. J. Barbour, *J. Am. Chem. Soc*., 2006, **128**, 698-699.
14 (a) CrysAlisPro CCD and RED, version 1.171.35.21, Oxford Diffraction, Ltd., Oxford, U.K., 2012; (b) G. M. Sheldrick, *Acta Crystallogr. A,* 2008, **64**, 112-122; (c) C. F. Macrae, I. J. Bruno, J. A. Chisholm, P. R. Edgington, P. McCabe, E. Pidcock, L. Rodriguez-Monge, R. Taylor, J. van de Streek, and P. A. Wood, *J. Appl. Crystallogr.*, 2008, **41**, 466-470; (d) http://www.povray.org/; (e) P. van der Sluis and A. L. Spek, *Acta Crystallogr. A*, 1990, **46**, 194-201.

CrystEngComm

ARTICLE

Table 1 Crystal data and details of the refinement parameters for the crystal structures.

Compound reference	**1**	**2a**	**2b**	**3b**	**4b**	**4c**
Chemical formula	$C_{34}H_{40}Ag_2N_8$ ·2(BF_4)	$C_{34}H_{40}Ag_2N_8$ ·2(BF_4) ·2(CH_3CN)	$C_{34}H_{40}Ag_2N_8$ ·2(BF_4) CH_3CN	$C_{34}H_{40}Ag_2N_8$ ·2(BF_4) $(CH_3)_2CO$	$C_{34}H_{40}Ag_2N_8$ ·2(BF_4) C_2H_5OH	$C_{34}H_{40}Ag_2N_8$ ·2(BF_4) C_2H_5OH
Formula weight	950.10	1032.21	991.15	1008.18	996.17	996.17
Crystal system	Triclinic	Triclinic	Triclinic	Triclinic	Triclinic	Monoclinic
Space group	*P*1	*P*1	*P*1	*P*1	*P*1	*C2/c*
T/K	100(2)	100(2)	100(2)	100(2)	100(2)	100(2)
λ/Å	0.71073	0.71073	0.71073	0.71073	0.71073	0.71073
a/Å	8.9739(7)	8.7304(7)	10.1464(11)	10.0370(5)	9.8865(5)	28.486(6)
b/Å	9.4407(6)	9.6666(9)	14.2825(14)	14.3332(6)	14.2717(8)	11.1491(14)
c/Å	11.7436(8)	13.3193(10)	15.3309(17)	15.4185(8)	15.4908(8)	28.309(6)
α/°	92.162(5)	96.972(7)	111.046(10)	111.125(4)	109.722(5)	90.00
β/°	96.638(6)	100.487(6)	97.101(9)	97.059(4)	96.569(4)	118.27(3)
γ/°	104.282(6)	104.709(7)	101.812(9)	100.307(4)	101.580(4)	90.00
V/Å^3	955.43(12)	1052.33(15)	1981.8(4)	1992.80(17)	1975.91(18)	7918(3)
Z	1	1	2	2	2	8
D_{calc}/g cm^{-3}	1.651	1.629	1.661	1.680	1.674	1.671
μ MoKα/mm^{-1}	1.101	1.008	1.066	1.063	1.071	1.069
No. of reflections measured	9149	15189	17972	23022	25028	22696
No. unique reflections (R_{int})	4118 (0.0245)	5062 (0.0442)	9706 (0.0462)	9473 (0.0343)	9305 (0.0347)	10160 (0.1185)
No. reflections with I > 2s(I)	3632	4095	6367	7202	7264	5273
No. refined parameters	292	320	521	531	544	574
R_1^a, wR_2^b values [$I > 2\sigma(I)$]	0.0500, 0.1235	0.0575, 0.1416	0.0575, 0.1281	0.0504, 0.1197	0.0662, 0.1768	0.1182, 0.2662
R_1^a, wR_2^b (all data)	0.0587, 0.1294	0.0767, 0.1574	0.1015, 0.1592	0.0745, 0.1386	0.0882, 0.1919	0.2012, 0.3345
Goodness-of-fit on F^2	1.092	1.082	1.020	1.069	1.092	1.040

[a] $R_1 = \sum \| F_o | - | F_c \| / \sum | F_o |$.

[b] $wR_2 = \{\sum[w(F_o^2 - F_c^2)^2] / \sum[w(F_o^2)^2]\}^{1/2}$.

CrystEngComm

ARTICLE

Graphical abstract

A few snapshots from a dynamic solvent diffusion process, through a seemingly non-porous crystal of a dinuclear, cyclic Ag(I) complex, were revealed. These indicate the complexity of the process, which involves not only relocation of the molecules in the crystal lattice, but also conformational adjustments of the metallocycles in response to solvent uptake/release. The transformations are reversible and do not cause the deterioration of the single-crystals, pointing out cooperativity of the molecules enclosed in the crystal unity.

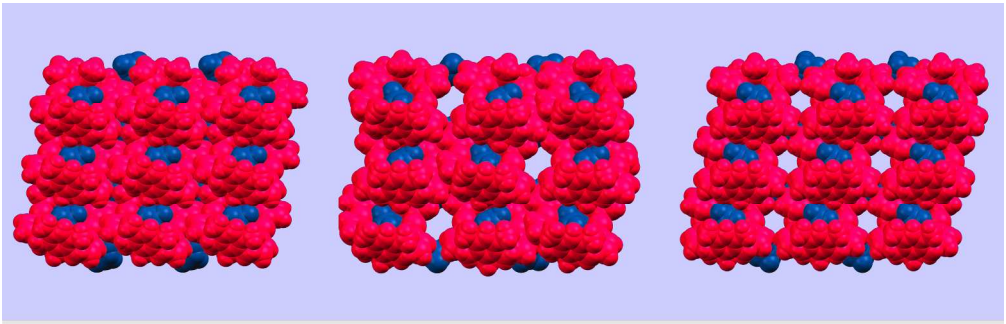

$[Ag_2L_2](BF_4)_2$ + solvent ⇌ - solvent ·acetonitrile ·ethanol ·acetone + solvent ⇌ - solvent ·2 acetonitrile ~~·2 ethanol~~ ~~·2 acetone~~